Torque Density Improvement of Concentrated Flux-type Synchronous Motor for Automotive Application

Jong-Hyun Park[1], Young-Hoon Jung[1], Kyung-Tae Jung[1], Myung-Hwan Yoon[1], Jung-Pyo Hong[1]
[1] Department of Automotive Engineering, Hanyang University, Seoul, 133-791, Korea, hongjp@hanyang.ac.kr

***Abstract*——— This paper proposes alternate bridge core of the Concentrated Flux-type Synchronous Motor (CFSM) using ferrite permanent magnets for automotive chassis actuator. The advantage of this structure is the reduction of leakage flux in the rotor bridges. Therefore, torque is enhanced in the safe mechanical structure. It is analyzed under the conditions of the constant volume of the PMs as well as the constant diameter of the rotor. By using the proposed method, the improved model is designed based on the initial model fulfilling the required specifications. Finally, the torque and mechanical characteristics of the two motors are simulated through the finite element analysis (FEA).**

Keywords— Alternate Bridge Core, Automotive Chassis Actuator, Concentrated Flux-type Synchronous Motor (CFSM), Ferrite Permanent Magnet, Mechanical Strength, Torque Density

I. INTRODUCTION

In the automotive industry there has been an increased emphasis on vehicle safety and environment. Improvement in automotive technology has greatly contributed to safety of vehicles and environment. Increased functionality has resulted in products like Electric Power Steering (EPS), Anti-lock Brake System (ABS), Adaptive Front Lighting System (AFLS), Electronic Stability Control (ESC) and automotive chassis application assist system. Furthermore, in an effort to continue this improvement in functionality and reduction in environmental impact, automotive components manufacturers and car manufacturers are developing electro-mechanical system, and demand for electric motor has increased significantly for automotive parts [1]-[3]. Nowadays, there are various types of permanent magnet synchronous motor (PMSM) applied to various automotive chassis application such as EPS, ABS, AFLS, ESC, electric booster, and etc. Most of motors as automotive actuator use the surface mounted PMSM (SPMSM). Because, it has relatively small size and simple rotor structure. However, SPMSM designed for automotive application usually has retainers in the rotor in order to prevent the scattering of permanent magnet (PM). This additional structure increases magnetic air-gap and then decreases torque density. In order to overcome such limitation of SPMSM, an interior permanent magnet synchronous motor (IPMSM) has been developed [4]. Also, IPMSM that uses rare-earth PM has attracted attention for its high power density. The IPMSM has higher power density than the SPMSM, because it can use a magnetic and a reluctance torque with current phase control method [5]. But recently, the prices of rare-earth PM have increased and they are also limited in exports [6]. To reduce dependence on rare-earth PM, various motors without rare-earth PM, such as induction motors, synchronous reluctance motor (SynRM), and Concentrated Flux-type Synchronous Motor (CFSM) are being developed [7]-[9]. Especially, ferrite PM is now being considered as a substitute for rare-earth PM Because of the situation mentioned above. Meanwhile, although the residual induction of ferrite PM is one-third of a rare-earth PM, the cost is only about one-tenth [7]-[12]. However, a stable supply of ferrite PM is available. In order to satisfy performance by using ferrite PM, it is necessary to improve the energy density by increasing the usage amount of the PM. There are various methods and types of motor to increase the usage of PM within a limited space. Among various methods, The CFSM is one of the most effective methods [13]-[14].

Most of previous research related to the CFSM using ferrite magnets did not consider design space and specification. However, the automotive chassis actuator should meet the output power in a limited design space and limited specification. The design space of actuator used in this study is shown in TABLE I. As can be seen in the table, in order to improve torque density under the limited condition, this paper propose that the CFSM with alternate bridge core is applied to design. The advantage of this design is the reduction of leakage flux in the rotor bridges. Therefore, torque density is enhanced in the safe mechanical structure. Hence, this paper deals with the analytical method and finite element analysis (FEA) to design the ferrite PM CFSM to enhanced torque density. At first, the initial model is designed by using the equivalent magnetic circuit of CFSM. Also, the tendency according to the pole angle is considered. Secondly, rotor core is replaced by alternate bridge core of the motor based on the proposed initial model. Finally, the back electromotive force (BEMF), the torque characteristics and mechanical characteristics of the two models are presented and compared by using FEA.

TABLE I. DESIGN SPECIFICATIONS

Parameter	*Unit*	*Value*
Stator outer diameter	mm	75
Stack length	mm	18
Rated torque	Nm	1.5
Rated speed	rpm	3,300
Input voltage (line to line)	V_{rms}	7.34
Limit current	A_{rms}	65
Connection	-	Delta

978-1-5090-4281-4/17/$31.00 ©2017 IEEE

II. INIRIAL MODEL USING EQUIVALENT MAGNETIC CIRCUIT

The electrical and mechanical power can be expressed by (1) based on the energy conservation law. If the current and angular velocity are constant, The BEMF and the torque are proportional. Therefore, it is reasonable to approach with the BEMF to find a model satisfying the rated torque .The equivalent circuit to find CFSM rotor parameters are presented.

$$\omega_m \cdot T = mei \tag{1}$$

where ω_m and T are mechanical angular speed in rad/s and torque in Nm respectively. m is the number of phase. e is the BEMF in V_{rms}. i is the input current in A_{rms}.

A. The equivalent magnetic circuit of CFSM

The geometry of CFSM used in this study is shown in Fig. 1. In the analytical model, the following assumptions are considered

- Saturation effects are not considered (with exception for the bridges) and the core permeability is considered infinite

- No even harmonics and only cosine harmonics

- The fringing effect is negligible

- The slot openings are not considered

- PM irreversible demagnetization is not considered, assuming PM with high coercive force and an adequate magnetic design

The stator slot openings are neglected, the air-gap is increased by means of the Carter factor k_{Cart}. Consequently, the effective air-gap is

$$g = k_{Cart} g_{act} \tag{2}$$

where g *and* g_{act} are the effective air-gap length and the actual air-gap in mm, respectively. k_{Cart} is the Carter factor.

The bridges are necessary for mechanical reason. However, due to the bridge structure, the flux remains in the rotor without crossing the air-gap. Geometry of the CFSM and the equivalent magnetic circuit considering the bridges are shown Fig. 1. and Fig. 2. Magnetomotive force of PM F_{PM} is

$$F_{PM} = \frac{B_{rem}}{\mu_0 \mu_{rec}} t_m \tag{3}$$

where B_{rem} is the residual induction in T. μ_0, and μ_{rec} are the permeability of free space and the recoil permeability of PM in H/m, respectively. t_m is the thickness of the PM in mm. The flux of PM Φ_{PM} is

$$\Phi_{PM} = \frac{F_{PM}}{R_m + (R_{bri} \,||\, R_g)} \tag{4}$$

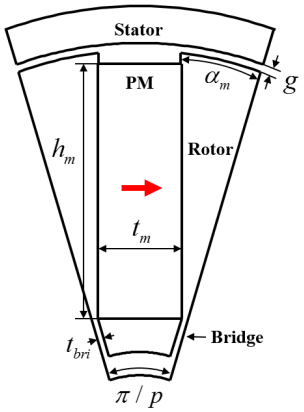

Fig. 1. Geometry of the CFSM for one pole used in the analytical approach.

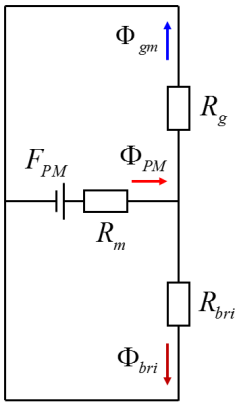

Fig. 2. The equivalent magnetic circuit of the CFSM.

The bridges leakage flux Φ_{bri} is

$$\Phi_{bri} = \frac{R_g}{R_{bri} + R_g} \Phi_{PM} \tag{5}$$

The air-gap flux Φ_{gm} is

$$\Phi_{gm} = \frac{R_{bri}}{R_{bri} + R_g} \Phi_{PM} \tag{6}$$

where R_m is the magnetic PM reluctance in A/Wb. R_{bri} and R_g are the bridge reluctance and the air-gap reluctance per one pole in A/Wb, respectively. The PM reluctance R_m is

$$R_m = \frac{t_m}{\mu_0 \mu_{rec} h_m L_{stk}} \tag{7}$$

The air-gap reluctance per one pole R_g is

$$R_g = \frac{2g}{\mu_0 \frac{\alpha_m D}{2p}} \tag{8}$$

and the bridge reluctance R_{bri} is

$$R_{bri} = \frac{2 \cdot l_{bri}}{\mu_0 \mu_r t_{bri} L_{stk}} \tag{9}$$

where μ_r is the relative permeability of the bridge. Specially, the permeability of bridges is calculated using the direct convergence method. D is the rotor outer diameter in mm. L_{stk} is the stack length of the rotor in mm, and. p is the number of pole-pair. α_m is half of pole arc in radian. t_m and h_m are the thickness and height of the PM in mm, respectively. l_{bri} and t_{bri} are the length of bridge and the thickness of bridge in mm, respectively.

Since the component contributing to the output power is considered the fundamental component of the air-gap flux density, only the fundamental component of the square wave will be considered. The amplitude of the fundamental component air-gap flux density is

$$\hat{B}_{gm1} = \frac{4}{\pi} \frac{2p\Phi_{gm}}{\alpha_m D} \sin \alpha_m \tag{10}$$

The fundamental component of the air-gap flux per one pole Φ_{gm1} is

$$\Phi_{gm1} = \frac{DL_{stk}}{p} \hat{B}_{gm1} \tag{11}$$

Based on (11), the BEMF E_a of the CFSM is calculated by considering the winding factor, turn number, and geometric dimensions. The derived equation is shown in (12).

$$E_a = \omega \Psi_m = \omega k_w N \Phi_{gm1} \tag{12}$$

where ω is the electrical angular speed in rad/s, and Ψ_m is the linkage flux in Wb. k_w is the winding factor, and N is the coil turn number. As a result, the equivalent magnetic circuit to determine CFSM rotor parameters are presented [15].

In the following section, initial design parameters are chosen to maximize the BEMF at the input voltage of the automotive actuator. The voltage drop due to the resistance and inductance 1is assumed to 20% margin of input voltage. (13) is the voltage equation of motor.

$$V = Ri + L\frac{di}{dt} + e \tag{13}$$

where V is the input voltage in V_{rms}. R is the phase resistance of the coil in ohm. L is the phase inductance in H. i and e are the phase current in A_{rms} and the BEMF in V_{rms}, respectively. The initial design is based on the BEMF using to the equivalent magnetic circuit and (11).

B. The effect of pole angle

A rotor tip structure is necessary to prevent scattering of PMs. As shown in Fig. 1. the pole angle is defined as the length of both ends of the rotor tips. The pole angle and the rotor tip vary at the same time. Fig. 3. is shown in the tendency of the phase BEMF according to the pole angle. Since the angle of the minimum pole angle is 24 degrees in order to prevent the scattering of the PMs, the pole angle is considered to be 24 degrees or more. Fig. 3. shows that the phase BEMF increases as the pole angle decreases. It is because related to leakage flux. Therefore, the electrical performance is better with smaller pole angle. The configurations of the motor are shown in Fig. 4(a). The thickness of the bridge is selected to be 0.5 mm for reasons of mold technology. The dimensions of the initial model are shown in TABLE II.

III. Replaced by Alternate Bridge Core

Because the automotive chassis actuator is designed in a limited space, it is necessary to reduce leakage flux which improves the output power of the motor. As a general method, there is a method of reducing leakage flux by using a non-magnetic material at a leakage path. Another method is to increases the air-gap flux density. Among the various methods, this paper propose alternate bridge core structure in order to reduce the leakage flux around the rotor inner circumference.

As shown in Fig. 4(b). The number of bridges is reduced by half and they are connected to the identical polarity. In this alternate bridge core model, since the leakage flux approaches zero, the amount of air-gap flux increases. In other words, As shown in the magnetic equivalent circuit of Fig. 2. and (6), neglecting the effects of bridges increases the air-gap flux density. Likewise, because the leakage path includes air-barrier, the reluctance is increased, as shown in Fig. 4(b). Therefore, torque density is enhanced.

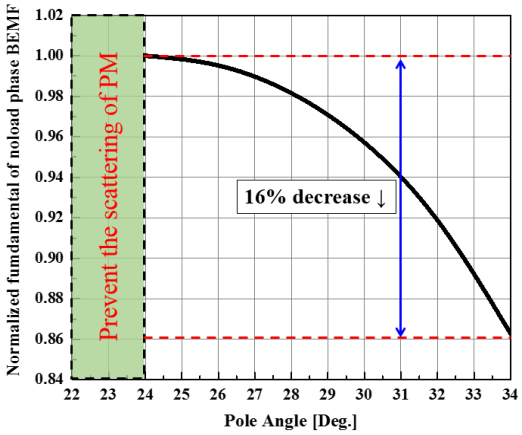

Fig. 3. The fundamental component of phase BEMF tendency according to pole anlge.

IV. Comparison of Initial Model and Alternate Bridge Core Model

It is analyzed under the conditions of the constant volume of PMs, the constant diameter of the rotor and identical stator. Comparisons are carried out between the two models, including the phase BEMF waveform, torque and mechanical strength characteristics.

A. No-load Characteristics

First, no-load phase BEMF waveform of the two models are investigated by FEA. Although the loading has great influences on the performance of motor, preliminary prediction can be made based on the open-circuit result.

As a result, the leakage flux is decreased and confirmed the result that the fundamental component of phase BEMF increased by 6.5% from 1.54 to 1.64 V_{rms} at rotation speed 1,000 rpm. The phase BEMF waveform can be obtained as shown in Fig. 5.

B. On-load Characteristics

The two models were investigated the influence of leakage flux in CFSM model with alternate bridge core, including the torque characteristics. With a line current 65A_{rms} rated current applied at rated speed 3,300 rpm and the current control method is $i_d = 0$. The torque characteristics can be obtained as shown in Fig. 6.

As a result, alternate bridge is applied by initial model under the same conditions, the average torque increased by 5% from 1.59 to 1.67 Nm at rated speed 3,300 rpm. As shown in (1), as the torque is improved, the input current can be lowered and the copper loss and core loss are reduced under the same torque condition.

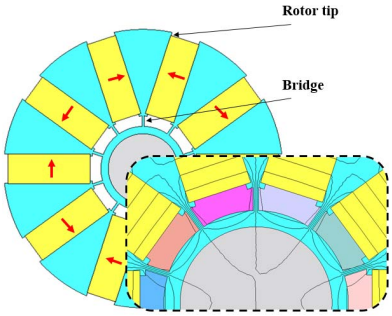

(a) Initial model

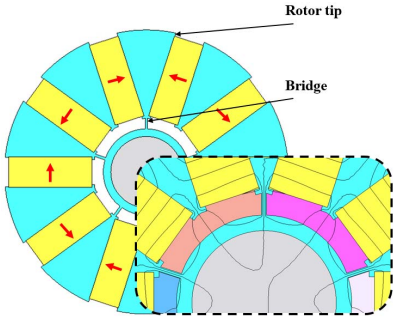

(b) Alternate bridge Core model

Fig. 4. The CFSM using ferrite PM for automotive chassis actuator (Stator part not shown)

TABLE II. Dimensions of Initial Model

Parameter	*Unit*	*Value*
Stator slot / Rotor pole	-	12 / 10
Stator outer diameter	mm	75
Stack length	mm	18
Rotor outer diameter	mm	56
Air-gap length	mm	0.5
Pole angle	degree	24
PM size	mm	16.5 × 6
PM residual induction (NMF-9G)	T	0.41
The number of series turns per phase	-	34

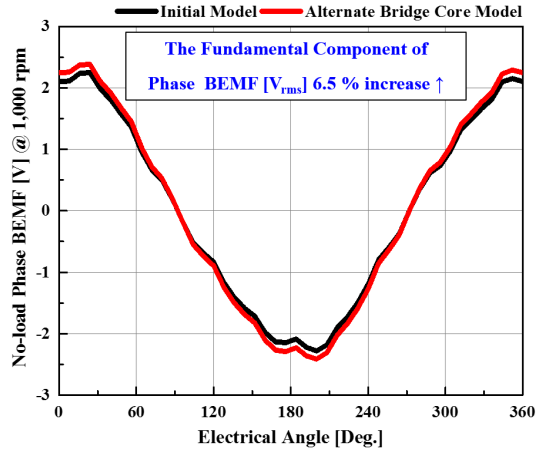

Fig. 5. The phase BEMF waveform comparison between initial model and alternate bridge core model.

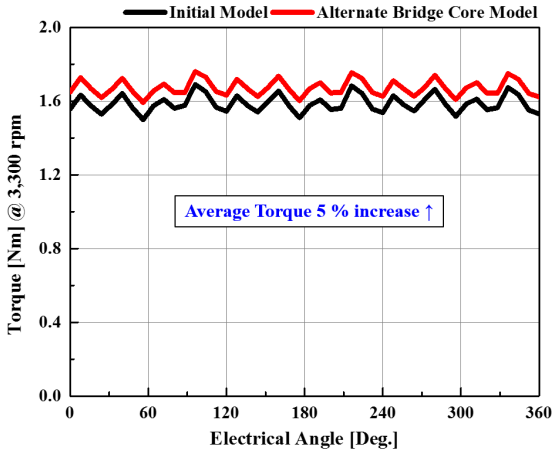

Fig. 6. The torque characteristics comparison between initial model and alternate bridge core model.

C. *Mechanical Strength Characteristics*

To verify the mechanical strength characteristics using FEA , the following assumptions are considered

- Steady-state speed conditions only

- Forces of electromagnetic origin are considered negligible

- Temperature effects are neglected

- Yield is indicated by planar Von Mises stress

- Vibration and rotor shaft dynamical forces are neglected

In order that the CFSM can operate in high speed region, the rotor mechanical strength should be ensured. If mechanical strength is not guaranteed, it will cause a serious problem such as scattering of the PMs and interference between rotor and stator. As shown in TABLE III, the 50PN470 is used as the material of the rotor core. The yield strength of 50PN470 is 275 MPa. In the analysis of the results, the maximum mechanical stress occurs in the rotor tip. Fig. 7. show stress distribution by using FEA.

In the initial model, the maximum stress is 20.7 MPa at the rotor tip and the safety factor is 13.3 at the speed of 5,000 rpm. The analysis condition 5,000 rpm reflected the safety factor 1.2 at the maximum speed. In addition, the stress in the alternate bridges is 17.3 MPa.

In the same analysis of the alternate bridge core model, the maximum stress is 43.9 MPa at the rotor tip and the safety factor is 6.26 at the speed of 5,000 rpm. Also, the stress in the alternate bridges is 31.6MPa. Therefore, a sufficient safety margin can be achieved, when compared with the yield strength. As a result, when changing from the initial model to the alternate bridge core model, the safety factor is lowered from 13.3 to 6.26. The mechanical characteristics are disadvantageous but the safety factor 6.62 of the alternate bridge core model can be judged to be stable. Therefore, the proposed model to improve the electrical performance is a reasonable configuration.

V. CONCLUSION

This paper propose that the CFSM with alternate bridge core is applied to design. The advantage of this design is the reduction of leakage flux in the rotor bridges. Therefore, torque density is enhanced in the safe mechanical structure. The proposed method is useful to design the CFSM to improve the torque density in a limited space of design.

Consequently, when applying the alternate bridge core, the fundamental component of phase BEMF increased by 6.5% from 1.54 to 1.64 V_{rms} at rotation speed 1,000 rpm and the average torque increased by 5% from 1.59 to 1.67 Nm at rated speed 3,300 rpm, compared to those of the initial motor. Finally, the maximum stress decreased from 20.7 MPa to 43.9 MPa at 5,000 rpm. The results of FEM are shown in TABLE IV. The alternate bridge core effect is analyzed by analytic method and validated by FEA.

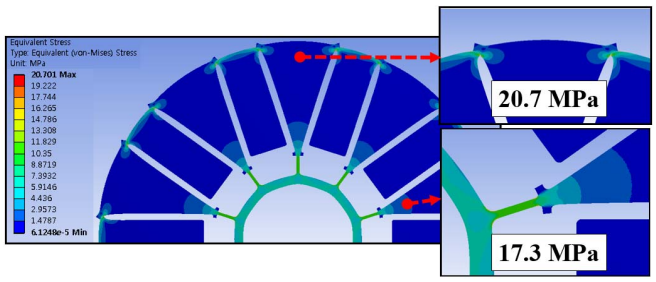

(a) Initial model

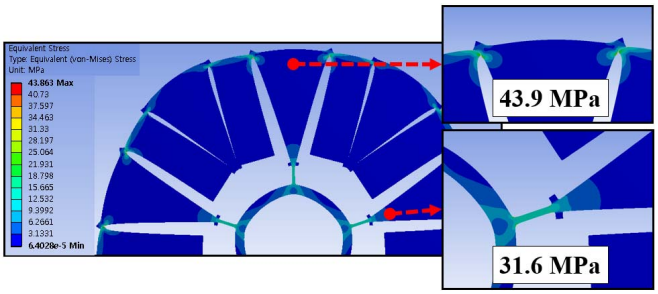

(b) Alternate bridge core model

Fig. 7. The stress distribution comparison between initial model and alternate bridge core model.

TABLE III. MATERIAL PROPERTY

Material	***Core (50PN470)***	***PM (NMF-9G)***
Density [kg/m3]	7,700	5,100
Young's Modulus [GPa]	180	150
Poisson's Ratio	0.30	0.25
Yield Strength [MPa]	275	276

TABLE IV. THE RESULTS OF FEA

	Initial Model	***Alternate bridge core Model***
The Fundamental Component of Phase BEMF [V_{rms}] @1,000 rpm	1.54	1.64 (6.5% ↑)
Average Torque [Nm] @ 3,300 rpm	1.59	1.67 (5% ↑)
Max. Stress [MPa] @ 5,000 rpm	20.7 (Safety factor 13.3)	43.9 (Safety factor 6.26)

ACKNOWLEDGMENT

This research was supported by the MSIP(Ministry of Science, ICT and Future Planning), Korea, under the ITRC(Information Technology Research Center) support program(IITP-2016-H8601-16-1005)supervised by the IITP(Institute for Information & communications Technology Promotion).

REFERENCES

[1] Tatsuya YAMASAKI, Masaaki EGUCHI, Yusuke MAKINO, "Development of an Electromechanical Brake," NTN TECHNICAL REVIEW, No.75, 2007.

[2] Myung-Seop Lim, Ji-Min Kim, Yong-Suk Hwang, and Jung-Pyo Hong, "Design of an Ultra-High Speed Permanent Magnet Motor for an Electric Turbocharger Considering Speed Response Characteristics," IEEE/ASME Trans. Mechatronics., Early Access Article, 2016.

[3] Myung-Seop Lim, Seung-Hee Chai and Jung-Pyo Hong, "Design and iron loss analysis of sensorless-controlled interior permanent magnet synchronous motors with concentrated winding," IET Electr. Power Appl., vol. 8, Iss. 9, pp. 349–356, 2014

[4] Myung-Seop Lim, Seung-Hee Chai, and Jung-Pyo Hong, "Design of Saliency-Based Sensorless-Controlled IPMSM With Concentrated Winding for EV Traction," IEEE Trans. Magn., vol. 52, no. 3, March 2016.

[5] Sung-Il Kim, Young-Kyoun Kim, Geun-Ho Lee and Jung-Pyo Hong, "A Novel Rotor Configuration and Experimental Verification of Interior PM Synchronous Motor for High-Speed Applications," IEEE Trans. Magn., vol. 48, no. 2, February 2012.

[6] Kodai Sone, Masatsugu Takemoto, Satoshi Ogasawara, Kenichi Takezaki, and Hidekatsu Akiyama, "A Ferrite PM In-Wheel Motor Without Rare Earth Materials for Electric City Commuters," IEEE Trans. Magn., vol. 48, no. 11, November 2012.

[7] Hae-Joong Kim, Doo-Young Kim, and Jung-Pyo Hong, "Structure of Concentrated-Flux-Type Interior Permanent-Magnet Synchronous Motors Using Ferrite Permanent Magnets," IEEE Trans. Magn., vol. 50, no. 11, November 2014.

[8] W. Kakihara, M. Takemoto, and S. Ogasawara, "Rotor structure in 50 kW spoke-type interior permanent magnet synchronous motor with ferrite permanent magnets for automotive applications," in *Proc. IEEE ECCE*, pp. 606–613, Sep. 2013.

[9] S.-I. Kim, J. Cho, S. Park, T. Park, and S. Lim, "Characteristics comparison of a conventional and modified spoke-type ferrite magnet motor for traction drives of low-speed electric vehicles," IEEE Trans. Ind. Appl., vol. 49, no. 6, pp. 3048–3054, Nov./Dec. 2013.

[10] A. Fasolo, L. Alberti, and N. Bianchi, "Performance comparison between switching-flux and IPM machine with rare earth and ferrite PMs," in Proc. 20th IEEE ICEM, Marseille, France, pp. 731–737 Sep. 2012.

[11] S. Ooi, S. Mormoto, M. Sanada, and Y. Inoue, "Performance evaluation of a high power density PMASynRM with ferrite magnets," IEEE Trans. Ind. Appl., vol. 49, no. 3, pp. 1308–1315, May/Jun. 2013.

[12] Min-Ro Park, Hae-Joong Kim, Yun-Yong Choi, Jung-Pyo Hong, and Jeong-Jong Lee, "Characteristics of IPMSM According to Rotor Design Considering Nonlinearity of Permanent Magnet," IEEE Trans. Magn., vol. 52, no. 3, March 2016.

[13] Kyu-Seob Kim, Min-Ro Park, Hae-Joong Kim, Seung-Hee Chai, and Jung-Pyo Hong, "Estimation of Rotor Type Using Ferrite Magnet Considering the Magnetization Process," IEEE Trans. Magn., vol. 52, no. 3, March 2016.

[14] Ji-Min Kim, Seung-Hee Chai, Myung-Hwan Yoon, and Jung-Pyo Hong, "Plastic Injection Molded Rotor of Concentrated Flux-Type Ferrite Magnet Motor for Dual-Clutch Transmission," IEEE Trans. Magn., vol. 51, no. 11, November 2015.

[15] Nicola Bianchi, Thomas M. Jahns, DESIGN, ANALYSIS, AND CONTROL OF INTERIOR PM SYNCHRONOUS MACHINES, 3rd ed., IEEE Industry Applications Society, 2004.